

This is the author's final, peer-reviewed manuscript as accepted for publication (AAM). The version presented here may differ from the published version, or version of record, available through the publisher's website. This version does not track changes, errata, or withdrawals on the publisher's site.

A high-performance open-source solution for multiphase fluid-structure interaction

Wendi Liu, Stephen M. Longshaw, Alex Skillen
and David R. Emerson

Published version information

Citation: W Liu et al. 'A high-performance open-source solution for multiphase fluid-structure interaction.' International Journal of Offshore and Polar Engineering 32, no. 1 (2022): 24-30.

DOI: [10.17736/ijope.2022.ic844](https://doi.org/10.17736/ijope.2022.ic844)

This version is made available in accordance with publisher policies. Please cite only the published version using the reference above. This is the citation assigned by the publisher at the time of issuing the AAM. Please check the publisher's website for any updates.

This item was retrieved from **ePubs**, the Open Access archive of the Science and Technology Facilities Council, UK. Please contact epublications@stfc.ac.uk or go to <http://epubs.stfc.ac.uk/> for further information and policies.

A High-performance Open-source Solution for Multiphase Fluid-structure Interaction

Wendi Liu, Stephen M. Longshaw, Alex Skillen and David R. Emerson
Scientific Computing Department, Science and Technology Facilities Council, Daresbury Laboratory
Warrington, United Kingdom

Carmine Valente and Francesco Gambioli
Airbus Operations Ltd.
Filton, Bristol, United Kingdom

A multiphase fluid-structure interaction (FSI) framework using open-source software has been developed, utilising components able to run on high-performance computing platforms. A partitioned approach is employed, ensuring a separation of concerns (fluid, structure, and coupling), allowing design flexibility and robustness while reducing future maintenance effort. Multiphase FSI test cases have been simulated and compared with published results and show good agreement. This demonstrates the ability of this multiphase FSI framework in simulating complex and challenging cases involving a free liquid surface.

KEY WORDS: Multiphase simulation, partitioned fluid-structure interaction, multiphysics-coupled modelling.

INTRODUCTION

An important phenomenon in a wide range of scientific and engineering disciplines is the interaction between multiphase flow and elastic structures, such as an aircraft wing with a sloshing fuel tank (Gambioli et al., 2019, 2020; Mastroddi et al., 2019, 2020; Titurus et al., 2019; Saltari et al., 2021) and the impact of ocean waves on elastic ocean structures (Gomes et al., 2020). Accurately simulating a multiphase fluid-structure interaction (FSI) can help reveal the mechanisms behind important and complex real-world phenomena, allowing for important design considerations, such as how to protect an elastic structure from fatigue or failure (Botha and Hindley, 2015) or how to achieve active/passive control of a system (Ducoin et al., 2012). There is significant demand to develop an efficient and open-source numerical tool for the investigation of such phenomena. Because of the nonlinear, time-dependent, and multiphysical nature of these various multiphase FSI problems, a simulation tool that is both robust and highly scalable (in parallel computing terms) is challenging. There are notable commercial FSI solvers. However, few of them can achieve both numerical robustness and high scalability while also being able to tackle multiphase FSI problems. Commercial software, such as ANSYS (Rao, 2003) and COMSOL (Curtis et al., 2013), provide fully coupled FSI simulations. Compared with commercial software, open-source codes have advantages in removing parallel scaling-related costs (among other benefits such as enabling the implementation of bespoke solvers or algorithms, as well as transparency).

Martínez-Ferrer et al. (2018) established an FSI simulation tool using OpenFOAM. Both fluid and structure domains were discretised with the finite volume method and solved with OpenFOAM using up to four CPU cores. Integrating both fluid and structural domains in a single library with a code-specific data mapping method is a good way to model multiphysics problems with two or three computational domains. However, in the long run, maintaining these codes and gradually adding more computational domains will be onerous work. It is also less flexible in dealing with problems that exceed the ability of any individual established code. Performance of the overall FSI solution is also limited by the scalability of the host codebase, whereas a partitioned approach allows individual components with the system to

be scaled according to their problem size, allowing for more optimal use of computing resources.

In this study, we aim to establish a new parallel partitioned multiphase FSI simulation framework using open-source codes. We adopt a partitioned approach, ensuring good use is made of existing open-source software while allowing design flexibility and reduced future maintenance efforts. For a partitioned approach, a stable and accurate coupling algorithm with good scalability and flexibility is required. Several key coupling libraries provide algorithms for FSI simulations, such as Comana (König et al., 2016), OpenFPCI (Hewitt et al., 2019), preCICE (Bungartz et al., 2016), and the multiscale universal interface (MUI) coupling library (Tang et al., 2015). The Comana code is not open source, and OpenFPCI is designed as a coupling framework between a specific structural code, ParaFEM (Smith et al., 2007), and OpenFOAM fluid solver. OpenFOAM is also act as a host in OpenFPCI. In this work, we employ the MUI library as the interface coupling tool between fluid and structure domains. It provides highly flexible domain couplings, as it allows an arbitrary number of codes to communicate with one another via the message passing interface (MPI) communications using a cloud of data points (rather than a mesh), combined with high-order interpolation schemes to facilitate data use between dissimilar methods or discretisation. MUI coupling utilities (CU) with FSI coupling algorithms have been developed to achieve a tight and stable coupling. OpenFOAM (Weller et al., 1998) and FEniCS (Alnæs et al., 2015) are adopted as the multiphase computational fluid dynamics (CFD) and computational structure mechanics (CSM) solvers, respectively. All three codes (i.e., MUI, FEniCS, and OpenFOAM) are equally important in this framework. Codes used for this multiphase FSI framework are known to perform well in high-performance computing (HPC) environments and are well validated in their respective problem domains (Hoffman et al., 2015; Skillen et al., 2018; Bnà et al., 2019).

Because of its partitioned design, several potential open-source CSM solvers are available for use in this framework. Four key examples are LibMesh (Kirk et al., 2006), MOOSE (Gaston et al., 2009), deal.II (Arndt et al., 2017), and FEniCS (Alnæs et al., 2015). All four libraries have a large user community. libMesh is a framework designed for parallel adaptive mesh refinement finite element applications. MOOSE uses the PETSc library (Abhyankar et al., 2018) and libMesh for the finite element discretization. deal.II is a library that supports a variety

of finite elements and can handle locally refined grids. FEniCS is a C++ library wrapped by a Python interface and allows users to use a concise mathematical form of code to express partial differential equations (Richardson and Wells, 2016). MOOSE, deal.II, and FEniCS are reported to have good scalability when using thousands of MPI tasks for large meshes (Arndt et al., 2017; Permann et al., 2020; Richardson and Wells, 2021). We have adopted FEniCS for the present framework as it has an automatic assembly function, making building new structural solvers relatively easy, and also because it interfaces its C++ core code with Python, which is easy to maintain and expand while keeping a strong parallel performance compared with other CSM solvers. As with the choice of CSM solver, there are several appropriate choices for the CFD solver. Given the desire to tackle problems with a free surface and multiple phases, the choice of method was reasonably reduced to the volume-of-fluid (VOF) approach or smoothed particle hydrodynamics (SPH). The interFoam solver from OpenFOAM was selected as the basis for this framework as it implements a well-validated incompressible multiphase VOF approach (Deshpande et al., 2012) and has a similarly flexible design to FEniCS, allowing for easy development of extended or new solvers. The parallel performance of OpenFOAM is difficult to quantify as it varies from solver to solver and is heavily problem dependent because of its use of static domain decomposition. However, although it is rarely best in class, it is acceptable for many problems and suitable for our use cases. For other problem types, a different CFD solver capable of capturing different physics or scaling better on large HPC systems may be more appropriate. The partitioned approach used allows for a simple exchange of solver in the future.

To ensure the overall performance of the partitioned coupled design, it is important that the method used to allow for intersolver communication does not become a bottleneck. In a previous study, we observed good parallel performance of the MUI coupling library on up to 9,000 MPI tasks for a synthetic problem with a similar communication pattern to that of FSI (Skillen et al., 2018). A series of benchmark tests on the MUI library has been carried out on the United Kingdom’s last national HPC system, ARCHER, showing the scope for scalability based purely on the communication overheads introduced by using this library (Longshaw et al., 2019). Fig. 1 shows the results of a 300-million-cell to 300-million-cell coupled case with a uniform 50/50 split of resources; this shows good parallel performance on up to 12,000 MPI tasks. The performance of the framework has also been demonstrated in our previous work (Liu et al., 2021b), which has shown acceptable scalability, with a parallel efficiency (i.e., speedup over number of MPI tasks) of 68% for 1,000 MPI tasks for FSI simulations using this framework.

In this paper, we demonstrate the coupling scheme and governing equations of the framework. A series of test cases are compared with published results to show the accuracy of the framework. Future work on the multiphase FSI framework is also identified and listed.

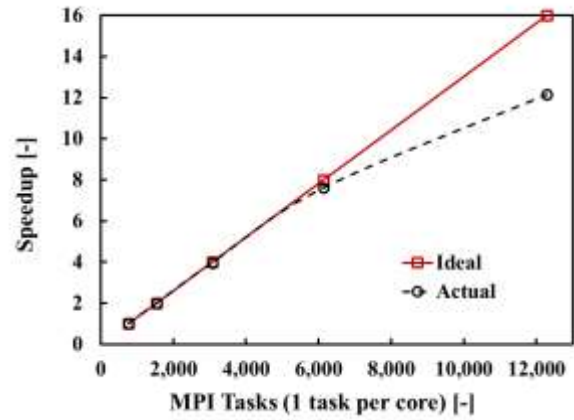


Fig. 1 Parallel performance of the MUI library

OPEN-SOURCE MULTIPHASE FSI FRAMEWORK

Fig. 2 shows the flowchart of the open-source multiphase FSI framework (Liu et al., 2021a). The left-hand side is the multiphase CFD solver (OpenFOAM v6) for the fluid domain, and the right-hand side is the CSM solver (FEniCS v2019.1.0) for the structural domain. The interface coupling tool (MUI v1.0) is in the middle.

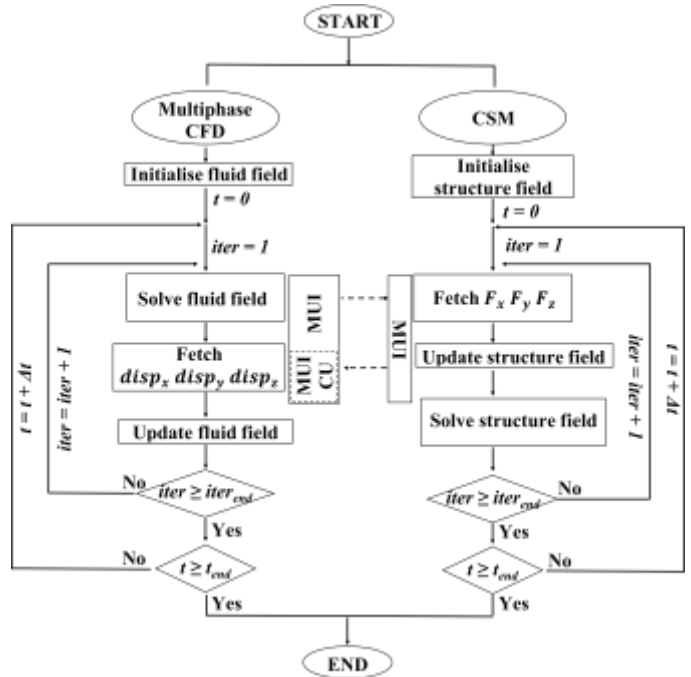


Fig. 2 Flowchart of the open-source framework with implicit FSI coupling scheme

Fluid Solver

The multiphase fluid solver interFSIFoam (Liu et al., 2021a) has been developed based on the standard OpenFOAM VOF solver interFoam. The interFSIFoam solver has the same core algorithms as interFoam for computation of the multiphase fluid domain in that it solves the incompressible Navier–Stokes equations with finite volume discretisation, using the VOF method to model the free surface. The continuity equation reads as (Tuković et al., 2018)

$$\nabla \cdot \mathbf{U} = 0, \quad (1)$$

where \mathbf{U} is the fluid velocity. The momentum equation over an arbitrary moving volume, which is due to the structure deformation, is stated as (Jasak, 2009; Tuković et al., 2018)

$$\frac{\partial \rho_f \mathbf{U}}{\partial t} + \nabla \cdot [\mathbf{U} \cdot \rho_f (\mathbf{U} - \mathbf{U}_s)] = -\nabla p + \nabla \cdot (\mu_f \nabla \mathbf{U}) + \mathbf{s}_\phi, \quad (2)$$

where ρ_f is the fluid density, t is the time, \mathbf{U}_s is the velocity of the surface S (i.e., the grid velocity), μ_f is the dynamic viscosity of the fluid, p is the fluid pressure, and \mathbf{s}_ϕ is the source term that includes both surface tension and gravity in the interFSIFoam solver. The space conservation law of the arbitrary Lagrangian-Eulerian (ALE) formulation that describes the relationship between the rate of change of the control volume V and the grid velocity \mathbf{U}_s is defined as

$$\frac{d}{dt} \int_V dV - \oint_S \mathbf{n} \cdot \mathbf{U}_s dS = 0, \quad (3)$$

where \mathbf{n} is the unit normal vector pointing outward of surface S . It is used to close the momentum equation with an arbitrary moving volume and is a built-in function of OpenFOAM (Jasak, 2009). The VOF method is used to model the free surface (Hirt and Nichols, 1981). Interfaces are constructed with the Multidimensional Universal Limiter for Explicit Solution (MULES) scheme. Artificial interface compressibility is employed in an attempt to prevent excessive numerical diffusion of the phase fraction field (Rusche, 2003). In our work herein, the extent of the interface compression is set conservatively such that spurious deformation of the interface is prevented while still being effective in reducing interface numerical diffusion. The OpenFOAM keyword “cAlpha” controls the extent of this compression and is set to the widely adopted value of 1 in all simulations presented herein. The $k-\epsilon$ turbulence model with wall functions are used to tackle the turbulence effect for the sloshing wing case. Additional functionalities of interFSIFoam when compared with the default OpenFOAM solver include (i) the calculation of fluid forces in each cell located at the interface between the fluid and structure domains, which are then sent to the structural solver; (ii) the ability to receive the displacement of each cell that is located in the interface between the fluid and structure domains and move the grid accordingly; and (iii) the conducting of subiterations for the fluid-structure interaction at each time step.

Structural Solver

The structural solver is developed using the libraries provided by the FEniCS framework, with governing equations discretised via the finite element method. The elastodynamics formulation can be expressed in the form of a generalised n -DOF (degrees of freedom) harmonic oscillator equation in terms of the body-fitted coordinates of the solid structure as

$$\mathbf{M} \frac{\partial^2 \mathbf{d}}{\partial t^2} + \mathbf{C} \frac{\partial \mathbf{d}}{\partial t} + \mathbf{K} \mathbf{d} = \mathbf{F}(t), \quad (4)$$

where \mathbf{M} is the mass matrix, \mathbf{C} is the damping matrix, \mathbf{K} is the stiffness matrix, \mathbf{F} is external loading and is a function of time, and \mathbf{d} is the deformation in respect to the body-fitted coordinates of the solid structure. In the presented solver, the damping matrix is modelled based on Rayleigh damping as

$$\mathbf{C} = \alpha_m \mathbf{M} + \alpha_k \mathbf{K}, \quad (5)$$

where α_m and α_k are Rayleigh damping parameters. Combining Eqs. 4 and 5 gives

$$\mathbf{M} \frac{\partial^2 \mathbf{d}}{\partial t^2} + (\alpha_m \mathbf{M} + \alpha_k \mathbf{K}) \frac{\partial \mathbf{d}}{\partial t} + \mathbf{K} \mathbf{d} = \mathbf{F}(t). \quad (6)$$

The generalised- α method, which is an extension of the Newmark- β

method (Newmark, 1959), is used to achieve a second-order accuracy for the time stepping (Erlicher et al., 2002; Bleyer, 2018). The generalised n -DOF harmonic oscillator equation is valid for small deformations of the structure.

Fluid-structure Interaction

The MUI code coupling library is used to create an interface between CFD and CSM codes. The fluid and structural domains of a partitioned FSI approach are coupled by kinematic and dynamic conditions at the interface where the domains meet. The displacement of the fluid-structure interface has to follow a kinematic condition to ensure consistency, whereas the fluid forces, or tractions, acting on the fluid-structure interface have to follow the dynamic condition to ensure conservation. The kinematic condition read as follows (Slyngstad, 2017):

$$\mathbf{d}_s = \mathbf{d}_f \quad (7)$$

where \mathbf{d}_s and \mathbf{d}_f represent the displacement at the fluid-structure interface in the structure and fluid domains, respectively. The consistency of the normal velocity at the fluid-structure interface is an alternative kinematic condition for fluid-structure coupling. In the present FSI framework, the consistency of the displacement is implemented, which is not as tight as the consistency of normal velocity, but is easier to implement. It is worth noting that employing consistency of the displacement as the kinematic condition has been validated and applied within numerous FSI studies (Slyngstad, 2017; Tao et al., 2018; Zhang et al., 2020). The fluid forces, or tractions, acting on the fluid-structure interface have to follow the dynamic condition (Slyngstad, 2017; Tuković et al., 2018):

$$\sigma_s \cdot \mathbf{n} = \mathbf{t}_f \quad (8)$$

where σ_s is the stress tensor of the structure domain, and \mathbf{t}_f is the traction at the fluid-structure interface, which is calculated as follows.

$$\mathbf{t}_f = \sigma_f \cdot \mathbf{n} \quad (9)$$

The stress tensor at the interface, σ_f , which is calculated from the fluid domain with an incompressible Newtonian fluid, is expressed as

$$\sigma_f = -p\mathbf{I} + \tau \quad (10)$$

where τ is the viscous component of the stress tensor, calculated as

$$\tau = \mu_f (\nabla \mathbf{U} + \nabla \mathbf{U}^T) \quad (11)$$

where the transpose of matrix \mathbf{A} is denoted as \mathbf{A}^T . The dynamic condition dictates that the forces acting on the fluid-structure interface have to be conserved between the two domains. This is achieved using the radial basis function (RBF) spatial interpolation method that is implemented within the MUI library. RBF spatial interpolation can handle general nonconformal meshes well regardless of gaps between meshes or different mesh densities (Rendall and Allen, 2008; Bungartz et al., 2016). The interpolation is based on radial basis functions established on each element/cell centre of the source mesh. Both Gaussian and Wendland's functions are available as the basis functions in MUI. At time step $t^{(n+1)} = t^n + \Delta t$ (where n is the number of time steps) and subiteration $(k+1)$ (where k is the subiteration number), the fluid domain solves the multiphase flow field to obtain the fluid forces. In this implementation, the fluid forces at each cell of the fluid-structure interface are transferred to the structural domain using MPI through the MUI library. The structural domain fetches fluid forces and applies them as the right-hand-side term of Eq. 6. It then calculates the deformation of the structure and pushes this information back to the fluid solver, again using MUI. The stress of the structure is then updated. The displacements of the structure in each cell of the interface are transferred and applied to the fluid domain as a Dirichlet boundary condition. Both fluid and structure domains are moved to the next

subiteration after the completion of these steps. Several such subiterations are needed within each time step until convergence is reached. Both fixed relaxation and Aitken's methods are employed here to achieve a tight coupling. The displacement of the structure at the $(k + 1)$ th iteration, \mathbf{d}_{k+1} , under the fixed-point Gauss-Seidel iteration method could be expressed as

$$\mathbf{d}_{k+1} = \mathbf{d}_k + \omega_k \mathbf{R}_k, \quad (12)$$

where ω_k is the underrelaxation factor at the k th iteration. The interface residual of the FSI coupling at the k th iteration, \mathbf{R}_k , is determined as

$$\mathbf{R}_k = \mathbf{F}_s \circ \mathbf{F}_f(\mathbf{d}_k) - \mathbf{d}_k, \quad (13)$$

where the \mathbf{F}_s and \mathbf{F}_f are the interface operators for structure and fluid, respectively; $a \circ b$ denotes a composite function of a composed with b ; that is, $a(b(x))$. For a fixed relaxation, fixed-point Gauss-Seidel iteration method, the underrelaxation factor can be expressed as

$$\omega_k = \text{constant}, \quad (14)$$

whereas for the Aitken's fixed-point Gauss-Seidel iteration method, the underrelaxation factor is calculated as

$$\omega_k = -\omega_{k-1} \frac{(\mathbf{R}_{k-1})^T (\mathbf{R}_k - \mathbf{R}_{k-1})}{\|\mathbf{R}_k - \mathbf{R}_{k-1}\|^2}. \quad (15)$$

A constraint can be applied to Aitken's method to make it stable, as follows:

$$\omega_k = \text{sgn}(\omega_k) \min(|\omega_k|, \omega_{\max}), \quad (16)$$

where ω_{\max} is the maximum value of the underrelaxation factors between the 1st and the k th iterations. The fixed relaxation method is easy to implement and requires fewer computational resources per subiteration, but it has a slow convergence speed. Aitken's method requires more computational resources per subiteration than the fixed relaxation method but has a quick convergence speed (Scheufele, 2015; Tuković et al., 2018). Both methods have been implemented here using MUI. A subiteration for FSI coupling is implemented in both solvers. In practice, the global time step size is set by ensuring that the CFL numbers based on fluid velocity, structure velocity, and the interface velocity are all smaller than their respective criteria according to their numerical methods. Both the CFD and the CSM solvers in the present framework always have the same time step size.

TEST CASES

Systematic verifications and validations have been carried out for the coupling between OpenFOAM and FEniCS using the MUI library with a single-phase fluid solver in previous work (Liu et al., 2021b). It covers both two-dimensional (2-D) and three-dimensional (3-D) aero/hydroelastic cases within both laminar and turbulence regimes. Good agreement with published numerical and experimental results has been achieved, which demonstrates the accuracy of the framework for cases with a single-phase fluid. In the present study, two test cases are presented here to verify the framework for multiphase FSI cases.

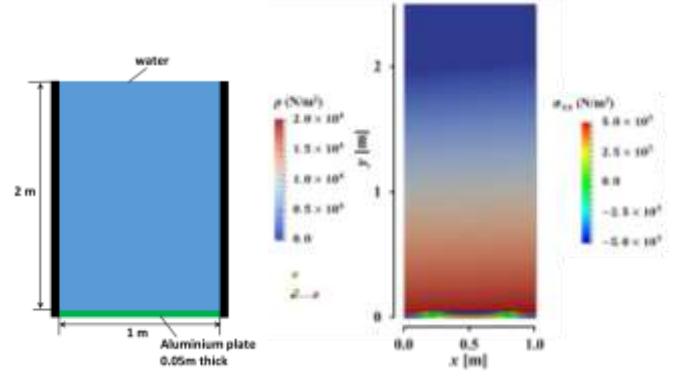


Fig. 3 Dimensions (left) and contour of the pressure field on the fluid domain and the x -axis normal stress field on the structure domain (right) of the hydrostatic water column on an elastic plate

The first is a 2-D hydrostatic water column on an elastic aluminium plate (Fourey et al., 2017; Khayyer et al., 2018). A steady water column with 2 m height and 1 m width is in a container. At the bottom, an elastic aluminium plate 1 m wide and 0.05 m thick is fixed at the sidewalls; this is shown in Fig. 3. The fluid domain is extended by 2.5 m in the y -axis direction, where the free surface between the air and water is located at $y = 2.0$ m. Although this is a 2-D test case, we have to specify the length of the plate along the third dimension (z -axis) in the CSM side because it is a 3-D solver. The length of the water column along the z -axis direction is consistent with that of the elastic plate. In the present test case, we set the length of the elastic plate and the water column along the z -axis direction to be the same as the thickness of the elastic plate (i.e., 0.05 m). It should be noted that different z -axis lengths result in different weights of water and natural frequencies of the elastic plate, but the displacement of the plate's midpoint will finally converge into the same value. The density, Young's modulus, and Poisson's ratio of the aluminium plate are $2,700 \text{ kg/m}^3$, $6.75 \times 10^{10} \text{ Pa}$, and 0.34, respectively. Following a convergence study, a 2-D structured grid with a high mesh density around the free surface, which contains approximately 25K cells, was employed for the fluid domain. The structural domain employed 4,620 DoF on the aluminium plate. Fig. 4 shows the time history of the vertical deformation of the aluminium plate's midpoint. After initial oscillations, the present simulation reached equilibrium. The results generated by the present simulation show good agreement with the analytical results from Fourey et al. (2017). The subplot of Fig. 4 shows the initial oscillations of the plate's midpoint compared with published results. A noticeable difference in the oscillation frequency between the present simulation and the published results can be observed, which should be caused by the different lengths of the tank and plate along the z -axis direction. The amplitude of the oscillation is qualitatively comparable with that of Khayyer et al. (2018). The contour plot of the pressure field on the fluid domain and the x -axis normal stress field on the structure domain at 1 s is shown in Fig. 3. It is comparable with that of Fourey et al. (2017) and Khayyer et al. (2018).

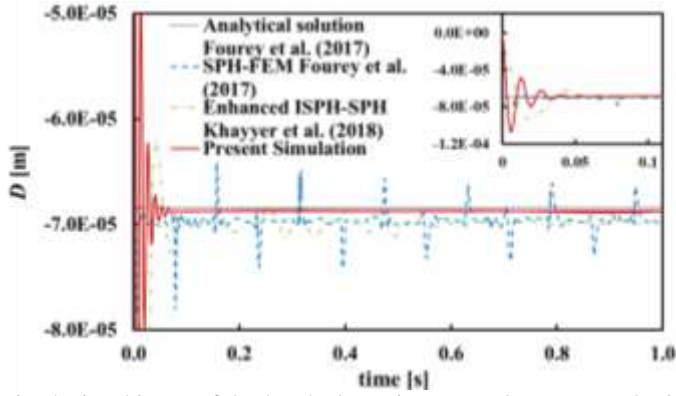


Fig. 4 Time history of the 2-D hydrostatic water column on an elastic plate for the instantaneous displacement of the plate's midpoint compared with published results (Fourey et al., 2017; Khayyer et al., 2018)

The second case comprises a partially filled roll tank with a clamped flexible beam in its centre. Results presented are compared directly with those already published. The test case is a two-dimensional roll tank with an elastic beam fixed at its middle bottom (Idelsohn et al., 2008; Paik and Carrica, 2014; Zhang et al., 2016). As shown in Fig. 5, the height of the tank is 0.3445 m, and the width is 0.609 m. The tank is filled with sunflower oil to a depth of 0.0574 m. The oil has a density of 917 kg/m^3 and kinematic viscosity of $5 \times 10^{-5} \text{ m}^2/\text{s}$. The flexible beam is constructed of dielectric polyurethane resin, with a height of 0.0574 m and width of 0.004 m. The density of the beam is $1,100 \text{ kg/m}^3$ and has a Young's modulus of $6 \times 10^6 \text{ Pa}$. The roll motion of the tank follows a sinusoidal function, with an amplitude of 4° and frequency of 0.61 Hz around the centre of the bottom of the tank.

As shown in Fig. 5, a 2-D mesh with a structured grid has been generated for the fluid domain; this contains approximately 0.6 million cells. The structural domain employs 3,075 DoF on the flexible beam. A convergence study has been done to ensure that the results are independent of the mesh size in both domains and the time step size is small enough to let the CFL number in the fluid domain be less than 1. The top boundary has a Dirichlet condition of 0 m/s for velocity components, with a fixed pressure of 0 Pa. All other boundaries are designated as nonslip walls. The fluid domain of this test case was solved with the body-fitted coordinates, meaning Eq. 2 becomes

$$\frac{\partial \rho_f \mathbf{U}_r}{\partial t} + \nabla \cdot [\mathbf{U}_r \cdot \rho_f (\mathbf{U}_r - \mathbf{U}_s)] = -\nabla p + \nabla \cdot (\mu_f \nabla \mathbf{U}_r) + \mathbf{s}_\phi, \quad (17)$$

where \mathbf{U}_r is the relative velocity in respect to the tank defined as

$$\mathbf{U}_r = \mathbf{U} - (\mathbf{r} - \mathbf{R}) \times \boldsymbol{\omega}(t), \quad (18)$$

where $\boldsymbol{\omega}$ is the angular velocity of any point in the tank and is a function of time, \mathbf{r} is the position vector, and the \mathbf{R} is the rotation centre. The results of the instantaneous displacement of the beam tip simulated by the present open-source multiphase FSI framework is shown in Fig. 6 and compared with published results. Idelsohn et al. (2008) carried out both experimental and numerical simulations that were based on the particle finite element method (PFEM) method. Paik and Carrica (2014) used the finite difference method (FDM) coupled with the finite element method (FEM) for the simulation. Finally, Zhang et al. (2016) obtained the results by using a framework made up of the moving particle semi-implicit (MPS) method coupled with FEM.

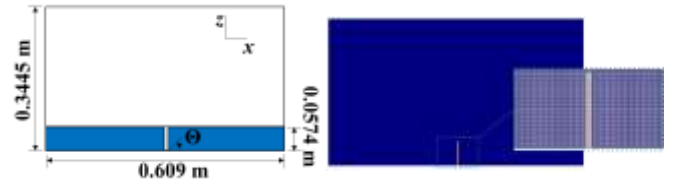


Fig. 5 Geometry and dimensions of the roll-tank case (left); fluid (blue) and structural (red) meshes of the roll tank with a clamped elastic beam (right)

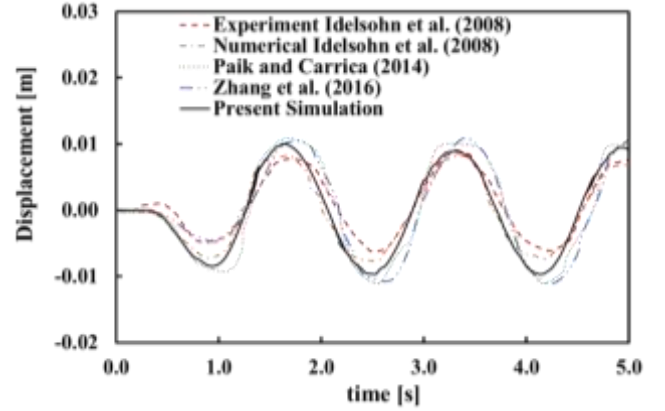


Fig. 6 Results of the roll tank with a clamped elastic beam case for the instantaneous displacement of the beam tip compared with published results (Idelsohn et al., 2008; Paik and Carrica, 2014; Zhang et al., 2016)

It can be seen that the displacement calculated by the present framework is close to the published numerical results. There are, however, discrepancies between the present simulation and the experiment. This may be, in part, due to the effect of the gap between the flexible beam and the tank walls, which is about 0.0029 m along the z -axis direction and cannot be captured within a 2-D simulation. In addition, the results presented are symmetrical, but the experimental results have a bias in the positive displacement direction. Fig. 7 shows results on the water phase contour at different time instants. Compared with that of Idelsohn et al. (2008) and Zhang et al. (2016), the elevation of the free surface calculated by the present framework is comparable with them both. The bubble cavity generated near the beam tip as the oil flows over the beam is reasonably close to that of Zhang et al. (2016) but, notably, was not obviously captured by the 3-D experiment.

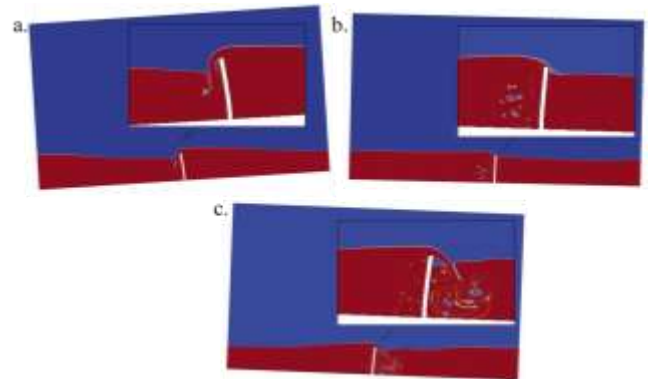


Fig. 7 Water phase contour of the rolling tank with an elastic beam with (a) $t = 0.92 \text{ s}$, (b) $t = 1.40 \text{ s}$, and (c) $t = 1.68 \text{ s}$

CONCLUSIONS

We have developed a preliminary multiphase FSI framework by using open-source codes with a partitioned approach. The high-performance and open-source MUI coupling library is employed as the interface between fluid and structure domains. OpenFOAM and FEniCS are adopted as the multiphase CFD and CSM solvers, respectively. FSI coupling algorithms have been implemented using the MUI library to achieve a tight and stable coupling. Test cases have been conducted and compared with published results that show good accuracy with the present multiphase FSI framework. Our ongoing work is to further enhance the performance of the framework toward an Exascale FSI computing platform, such as to implement dynamic load balancing on a per-solver basis and implement the use of elastic HPC resource per-solver and inherent communication-minimising algorithms within the coupling layer operating separately from the solver parallelisation.

At present, the multiphase FSI framework uses a global time step size, meaning both the CFD and the CSM solvers always have the same time step size. This scheme works well in the case where the time step sizes required by the CFD and CSM solvers are of the same order. However, when these are of different orders of magnitude, the present scheme is feasible but computationally costly. A more efficient way to simulate such a case is to implement an asynchronous time marching scheme, in which the fluid and structure domains have different time step sizes. In this time marching scheme, data exchange will not happen every time step but only when the solver with the larger time step size updates its results. This is currently being implemented in the presented framework.

ACKNOWLEDGEMENTS

This work was supported by the Sloshing Wing Dynamics (SLOWD) project. The SLOWD project has received funding from the European Union's Horizon 2020 research and innovation programme under Grant Agreement No. 815044. Parts of this work have been funded under the ARCHER2 embedded CSE programme of the ARCHER2 UK National Supercomputing Service (<https://www.archer2.ac.uk>).

REFERENCES

- Abhyankar, S, Brown, J, Constantinescu, EM, Ghosh, D, Smith, BF, and Zhang, H (2018). "PETSc/TS: A Modern Scalable ODE/DAE Solver Library," Preprint, submitted June 4, <https://arxiv.org/abs/1806.01437>.
- Alnæs, M, Blechta, J, Hake, J, Johansson, A, Kehlet, B, Logg, A, Richardson, C, Ring, J, Rognes, ME, and Wells, GN (2015). "The FEniCS Project Version 1.5," *Arch Numer Software*, 3(100), 9–23.
- Arndt, D, Bangerth, W, Davydov, D, Heister, T, Heltai, L, Kronbichler, M, Maier, M, Pelteret, JP, Turcksin, B, and Wells, D (2017). "The Deal. II Library, Version 8.5," *J Numer Math*, 25(3), 137–145.
- Bleyer, J (2018). *Numerical Tours of Computational Mechanics with FEniCS*, access date: 12th Feb 2020, available at <https://comet-fenics.readthedocs.io/en/latest/intro.html>.
- Bnà, S, Spisio, I, Rossi, G, and Olesen, M (2019). "HPC Performance Improvements for OpenFOAM Linear Solvers," *7th ESI OpenFOAM Conf 2019*, Berlin, Germany, sponsor organization: ESI Group, 1-9.
- Botha, M, and Hindley, MP (2015). "One-way Fluid Structure Interaction Modelling Methodology for Boiler Tube Fatigue Failure," *Eng Fail Anal*, 48, 1–10.
- Bungartz, H-J, Lindner, F, Gatzhammer, B, Mehl, M, Scheufele, K, Shukaev, A, and Uekermann, B (2016). "preCICE—A Fully Parallel Library for Multi-physics Surface Coupling," *Comput Fluids*, 141, 250–258.
- Curtis, FG, Ekici, K, and Freels, JD (2013). "Fluid-structure Interaction Modeling of High-aspect Ratio Nuclear Fuel Plates Using COMSOL Multiphysics," *Proc 2013 COMSOL Conf*, Boston, MA, USA, sponsor organization: COMSOL, Inc., 1-36.
- Deshpande, SS, Anumolu, L, and Trujillo, MF (2012). "Evaluating the Performance of the Two-phase Flow Solver interFoam," *Comput Sci Discovery*, 5(1), 014016.
- Ducoin, A, Astolfi, JA, and Sigrist, JF (2012). "An Experimental Analysis of Fluid Structure Interaction on a Flexible Hydrofoil in Various Flow Regimes including Cavitating Flow," *Eur J Mech B Fluids*, 36, 63–74.
- Erlicher, S, Bonaventura, L, and Bursi, OS (2002). "The Analysis of the Generalized- α Method for Non-linear Dynamic Problems," *Comput Mech*, 28(2), 83–104.
- Fourey, G, Hermange, C, Le Touzé, D, and Oger, G (2017). "An Efficient FSI Coupling Strategy between Smoothed Particle Hydrodynamics and Finite Element Methods," *Comput Phys Commun*, 217, 66–81.
- Gamboli, F, Alegre Usach, R, Kirby, J, Wilson, T, and Behruzi, P (2019). "Experimental Evaluation of Fuel Sloshing Effects on Wing Dynamics," *Int Forum Aeroelasticity Struct Dyn*, Savannah, GA, USA, sponsor organization: Journal of Aeroelasticity and Structural Dynamics, 1–14.
- Gamboli, F, Chamos, A, Jones, S, Guthrie, P, Webb, J, Levenhagen, Behruzi, P, Mastroddi, F, Malan, A, and Longshaw, S (2020). "Sloshing Wing Dynamics—Project Overview," *Proc TRA2020 8th Transport Res Arena*, Helsinki, Finland, Traficom, Abstract 1024, pp 207-207, Published by Finnish Transport and Communications Agency Traficom.
- Gaston, D, Newman, C, Hansen, G, and Lebrun-Grandie, D (2009). "MOOSE: A Parallel Computational Framework for Coupled Systems of Nonlinear Equations," *Nucl Eng Des*, 239(10), 1768–1778.
- Gomes, RPF, Gato, LMC, Henriques, JCC, Portillo, JCC, Howey, BD, Collins, KM, Hann, MR, and Greaves, DM (2020). "Compact Floating Wave Energy Converters Arrays: Mooring Loads and Survivability through Scale Physical Modelling," *Appl Energy*, 280, 115982.
- Hewitt, S, Margetts, L, Revell, A, Pankaj, P, and Levrero-Florencio, F (2019). "OpenFPCI: A Parallel Fluid–structure Interaction Framework," *Comput Phys Commun*, 244, 469–482.
- Hirt, CW, and Nichols, BD (1981). "Volume of Fluid (VOF) Method for the Dynamics of Free Boundaries," *J Comput Phys*, 39(1), 201–225.
- Hoffman, J, Jansson, J, and Jansson, N (2015). "FEniCS-HPC: Automated Predictive High-performance Finite Element Computing with Applications in Aerodynamics," *11th Int Conf Parallel Process Appl Math*, Krakow, Poland, Springer, 356–365.
- Idelsohn, SR, Marti, J, Souto-Iglesias, A, and Oñate, E (2008). "Interaction between an Elastic Structure and Free-surface Flows: Experimental versus Numerical Comparisons Using the PFEM," *Comput Mech*, 43, 125–132.
- Jasak, H (2009). "Dynamic Mesh Handling in OpenFOAM," *47th AIAA Aerosp Sci Meet Incl New Horiz Forum Aerosp Exposition*, Orlando, FL, USA, sponsor organization: AIAA, 341.
- Khayyer, A, Gotoh, H, Falahaty, H, and Shimizu, Y (2018). "An Enhanced ISPH–SPH Coupled Method for Simulation of Incompressible Fluid–elastic Structure Interactions," *Comput Phys Commun*, 232, 139–164.
- Kirk, BS, Peterson, JW, Stogner, RH, and Carey, GF (2006). "libMesh: A C++ Library for Parallel Adaptive Mesh Refinement/coarsening Simulations," *Eng Comput*, 22(3–4),

- König, M, Radtke, L, and Düster, A (2016). "A Flexible C++ Framework for the Partitioned Solution of Strongly Coupled Multifield Problems," *Comput Math Appl*, 72(7), 1764–1789.
- Liu, W, Skillen, A, and Longshaw, S (2021a). *ParaSiF—Parallel Partitioned Multi-physics Simulation Framework*, access date: 5th Jul 2021, available at <https://github.com/ParaSiF/ParaSiF>.
- Liu, W, Wang, W, Skillen, A, Longshaw, S, Moulinec, C, and Emerson, D (2021b). "Parallel Partitioned Approach On Fluid-structure Interaction Simulations Using the Multi-scale Universal Interface Coupling Library," *14th WCCM-ECCOMAS Congr*, Virtual, Online, Published by SCIPEDIA, Volume 1400, pp 1-12.
- Longshaw, SM, Pillai, R, Gibelli, L, Emerson, DR, and Lockerby, DA (2019). "Multiscale Simulation of Evaporation Using the Multiscale Universal Interface," *31st Int Conf Parallel Comput Fluid Dyn*, Antalya, Turkey, sponsor organization: METU, pp 1-1 .
- Martínez-Ferrer, PJ, Qian, L, Ma, Z, Causon, DM, and Mingham, CG (2018). "An Efficient Finite-volume Method to Study the Interaction of Two-phase Fluid Flows with Elastic Structures," *J Fluids Struct*, 83, 54–71.
- Mastroddi, F, Saltari, F, Traini, A, Barile, A, and Gambioli, F (2020). "Sloshing ROMs for Fluid-structure Interactions in Aerospace Applications," *AIAA Scitech 2020 Forum*, Orlando, FL, USA, American Institute of Aeronautics and Astronautics, sponsor organization: AIAA 2020-1451.
- Mastroddi, F, Saltari, F, Wright, M, Malan, AG, Simeone, S, and Gambioli, F (2019). "Aircraft-fuel Sloshing ROMs for Aeroelastic Analyses," *Int Forum Aeroelasticity Struct Dyn*, Savannah, GA, USA, sponsor organization: Journal of Aeroelasticity and Structural Dynamics, 9–13.
- Newmark, NM (1959). "A Method of Computation for Structural Dynamics," *J Eng Mech Div*, 85(3), 67–94.
- Paik, K-J, and Carrica, PM (2014). "Fluid–structure Interaction for an Elastic Structure Interacting with Free Surface in a Rolling Tank," *Ocean Eng*, 84, 201–212.
- Permann, CJ, Gaston, DR, Andrš, D, Carlsen, RW, Kong, F, Lindsay, AD, Miller, JM, Peterson, JW, Slaughter, AE, Stogner, RH and Martineau, RC (2020). "MOOSE: Enabling Massively Parallel Multiphysics Simulation," *SoftwareX*, 11, 100430.
- Rao, A (2003). "Fluid–solid Interaction Analysis Using ANSYS/multiphysics," *Proc 2nd MIT Conf Comput Fluid Solid Mech*, Cambridge, MA, USA, published by Elsevier, 1492–1496.
- Rendall, TC, and Allen, CB (2008). "Unified Fluid–structure Interpolation and Mesh Motion Using Radial Basis Functions," *Int J Numer Methods Eng*, 74(10), 1519–1559.
- Richardson, CN, and Wells, GN (2016). *High Performance Multi-Physics Simulations with FEniCS/DOLFIN*, eCSE03-10 Report, ARCHER, available at [figshare](https://doi.org/10.6084/m9.figshare.3406582.v3), <https://doi.org/10.6084/m9.figshare.3406582.v3>.
- Rusche, H (2003). *Computational Fluid Dynamics of Dispersed Two-phase Flows at High Phase Fractions*, Doctoral dissertation, Imperial College London, London, 666 pp.
- Saltari, F, Traini, A, Gambioli, F, and Mastroddi, F (2021). "A Linearized Reduced-order Model Approach for Sloshing to Be Used for Aerospace Design," *Aerosp Sci Technol*, 108, 106369.
- Scheufele, K (2015). *Robust Quasi-Newton Methods for Partitioned Fluid-structure Simulations*, Master's thesis, University of Stuttgart, Stuttgart, Germany, 95 pp.
- Skillen, A, Longshaw, SM, Cartland-Glover, G, Moulinec, C, and Emerson, DR (2018). "Profiling and Application of the Multi-scale Universal Interface (MUI)," *7th Eur Conf Comput Fluid Dyn*, Glasgow, UK, sponsor organization: UKACM, 1-8.
- Slyngstad, AS (2017). *Verification and Validation of a Monolithic Fluid-structure Interaction Solver in FEniCS: A Comparison of Mesh Lifting Operators*, Master's thesis, University of Oslo, Oslo, Norway, 68 pp.
- Smith, IM, Margetts, L, Beer, G, and Dünser, C (2007). "Parallelising the Boundary Element Method Using ParaFEM," *Proc 10th Int Conf Numer Methods Geomech*, Rhodes, Greece, Published by CRC Press, 177-181 .
- Tang, Y-H, Kudo, S, Bian, X, Li, Z, and Karniadakis, GE (2015). "Multiscale Universal Interface: A Concurrent Framework for Coupling Heterogeneous Solvers," *J Comput Phys*, 297, 13–31.
- Tao, W, Guo, Y, He, Z, and Peng, X (2018). "Investigation on the Delayed Closure of the Suction Valve in the Refrigerator Compressor by FSI Modeling," *Int J Refrig*, 91, 111–121.
- Titurus, B, Cooper, JE, Saltari, F, Mastroddi, F, and Gambioli, F (2019). "Analysis of a Sloshing Beam Experiment," *Int Forum Aeroelasticity Struct Dyn*, Savannah, GA, USA, sponsor organization: Journal of Aeroelasticity and Structural Dynamics, Volume 139.
- Tuković, Ž, Karač, A, Cardiff, P, Jasak, H, and Ivanković, A (2018). "OpenFOAM Finite Volume Solver for Fluid-solid Interaction," *Trans FAMENA*, 42(3): 1–31.
- Weller, HG, Tabor, G, Jasak, H, and Fureby, C (1998). "A Tensorial Approach to Computational Continuum Mechanics Using Object-oriented Techniques," *Comput Phys*, 12(6), 620–631.
- Zhang, L, Yin, G, Wang, S, and Guan, C (2020). "Study on FSI Analysis Method of a Large Hydropower House and Its Vortex-induced Vibration Regularities," *Adv Civ Eng*, 2020(6), 7596080.
- Zhang, YL, Tang, ZY, and Wan, DC (2016). "MPS-FEM Coupled Method for Interaction between Sloshing Flow and Elastic Structure in Rolling Tanks," *Proc 7th Int Conf Comput Methods*, Berkeley, CA, USA, sponsor organization: University of California at Berkeley, 1–4.